

Symmetry Supported Magnetic Blocking at 20 K in the Pentagonal Bipyramidal Dy(III) Single-Ion Magnets

Yan-Cong Chen¹, Jun-Liang Liu^{1*}, Liviu Ungur^{2,3*}, Jiang Liu¹, Quan-Wen Li¹, Long-Fei Wang¹, Zhao-Ping Ni,¹ Liviu F. Chibotaru², Xiao-Ming Chen¹ and Ming-Liang Tong^{1*}

¹ Key Laboratory of Bioinorganic and Synthetic Chemistry of Ministry of Education, School of Chemistry and Chemical Engineering, Sun Yat-Sen University, Guangzhou 510275, P. R. China

² Theory of Nanomaterials Group and INPAC—Institute of Nanoscale Physics and Chemistry, Katholieke, Universiteit Leuven, Celestijnenlaan 200F, 3001 Leuven, Belgium

³ Theoretical Chemistry, Lund University, Getingeavagen 60, 22241, Lund, Sweden

*E-mail: tongml@mail.sysu.edu.cn, ljliang1987@gmail.com, Liviu.Ungur@chem.kuleuven.be

Contents

1. Crystal Data and Structures	S2
2. Magnetic Characterization	S6
3. Ab Initio Calculations	S9

1. Crystal Data and Structures

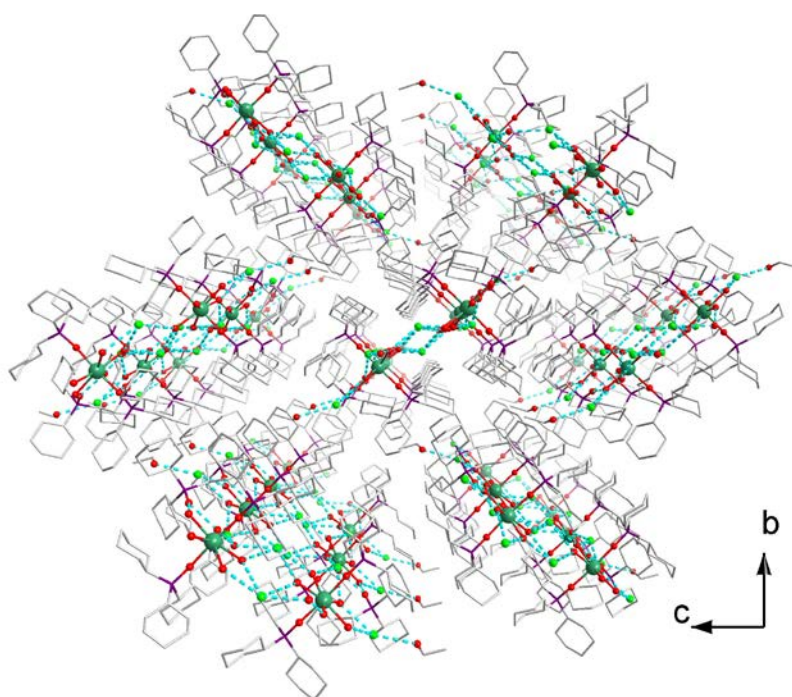


Figure S1. Crystal Structure of 1 viewed along the *a* axis. The dashed lines represent the intermolecular hydrogen bonds. H atoms are omitted for clarity. Color Codes: Dy, cyan; P, purple; Cl, green; O, red; C, gray; H, light gray.

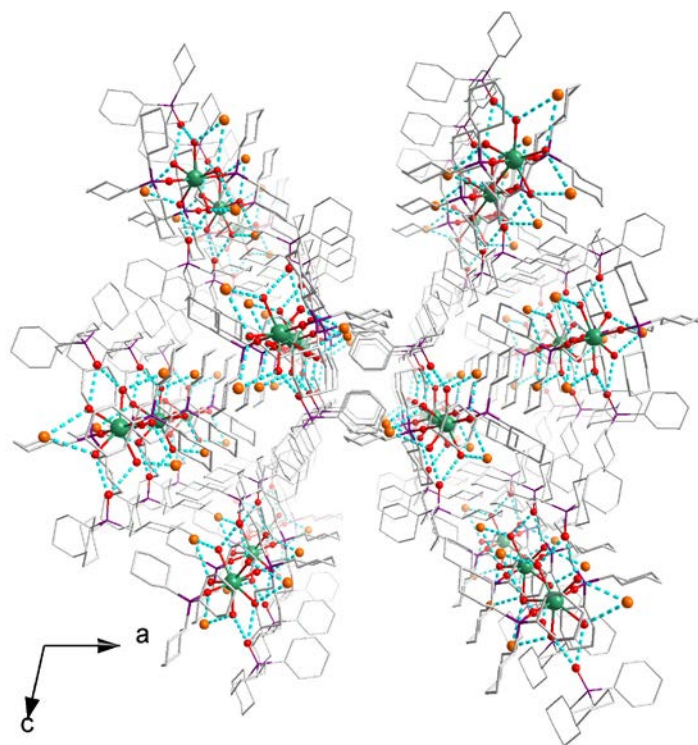


Figure S2. Crystal Structure of 2 viewed along the *b* axis. The dashed lines represent the intermolecular hydrogen bonds. H atoms are omitted for clarity. Colour Codes: Dy, cyan; P, purple; Br, orange; O, red; C, gray; H, light gray.

Table S1. Continuous Shape Measures calculations (CShM) for **1** and **2**.^a

Complex	HP-7 (<i>D</i> _{7h})	HPY-7 (<i>C</i> _{6v})	PBPY-7 (<i>D</i> _{5h})	COC-7 (<i>C</i> _{3v})	CTPR-7 (<i>C</i> _{2v})	JPBPY-7 (<i>D</i> _{5h})	JETPY-7 (<i>C</i> _{3v})
1	34.017	24.503	0.239	7.576	5.906	2.833	22.8
2	34.004	25.379	0.142	7.752	5.809	2.642	24.233

HP-7 = Heptagon; HPY-7 = Hexagonal pyramid; PBPY-7 = Pentagonal bipyramid; COC-7 = Capped octahedron; CTPR-7 = Capped trigonal prism; JPBPY-7 = Johnson pentagonal bipyramid J13; JETPY-7 = Johnson elongated triangular pyramid J7.
^a (a) Alvarez, S.; Alemany, P.; Casanova, D.; Cirera, J.; Llunell, M.; Avnir, D. *Coord. Chem. Rev.*, **2005**, *249*, 1693-1708; (b) Casanova, D.; Llunell, M.; Alemany, P.; Alvarez, S. *Chem. Eur. J.*, **2005**, *11*, 1479-1494.

Table S2. Crystal Data and Structural Refinements for **1** and **2**.

Complex	1	2
Chemical formula	C ₅₆ H ₁₁₇ Cl ₃ DyO ₁₀ P ₃	C ₇₂ H ₁₄₂ Br ₃ DyO ₉ P ₄
Formula Mass	1312.26	1677.97
Crystal system	Monoclinic	Monoclinic
<i>a</i> /Å	11.7472(5)	40.4082(15)
<i>b</i> /Å	29.5882(11)	14.2356(7)
<i>c</i> /Å	19.4338(8)	33.0134(14)
<i>β</i> /°	97.434(2)	102.6630(10)
Unit cell volume/Å ³	6698.0(5)	18528.5(14)
Temperature/K	150(2)	150(2)
Space group	<i>P</i> 2 ₁ / <i>n</i>	<i>C</i> 2/ <i>c</i>
No. of formula units per unit cell, <i>Z</i>	4	8
Radiation type	MoK _α	MoK _α
Absorption coefficient, μ/mm ⁻¹	1.356	2.213
No. of reflections measured	40418	59069
No. of independent reflections	12926	18082
<i>R</i> _{int}	0.1189	0.0747
<i>R</i> ₁ ^a (<i>I</i> > 2σ(<i>I</i>))	0.0605	0.0545
<i>wR</i> ₂ ^b (all data)	0.1324	0.1342
Goodness of fit on <i>F</i> ²	1.018	1.064

$$^a R_1 = \frac{\sum ||F_o| - |F_c||}{\sum |F_o|}$$

$$^b wR_2 = [\sum w(F_o^2 - F_c^2)^2 / \sum w(F_o^2)^2]^{1/2}$$

Table S3. Crystal Data and Structural Refinement for **1@Y** and **2@Y**.

Complex	1@Y	2@Y
Chemical formula	C ₅₆ H ₁₁₇ Cl ₃ Dy _{0.05} O ₁₀ P ₃ Y _{0.95}	C ₇₂ H ₁₄₂ Br ₃ Dy _{0.05} O ₉ P ₄ Y _{0.95}
Formula Mass	1242.35	1608.06
Crystal system	Monoclinic	Monoclinic
<i>a</i> /Å	11.7525(8)	40.347(3)
<i>b</i> /Å	29.615(2)	14.3228(11)
<i>c</i> /Å	19.4336(15)	33.253(2)
<i>β</i> /°	97.389(2)	102.448(2)
Unit cell volume/Å ³	6707.8(9)	18764(2)
Temperature/K	150(2)	150(2)
Space group	<i>P</i> 2 ₁ / <i>n</i>	<i>C</i> 2/ <i>c</i>
No. of formula units per unit cell, <i>Z</i>	4	8
Radiation type	MoK _α	MoK _α
Absorption coefficient, μ/mm ⁻¹	1.122	2.019
No. of reflections measured	41947	62011
No. of independent reflections	12943	18323
<i>R</i> _{int}	0.0925	0.1048
<i>R</i> ₁ ^a (<i>I</i> > 2σ(<i>I</i>))	0.0569	0.0596
<i>wR</i> ₂ ^b (all data)	0.1476	0.1457
Goodness of fit on <i>F</i> ²	1.063	0.978

$$^a R_1 = \frac{\sum ||F_o| - |F_c||}{\sum |F_o|}$$

$$^b wR_2 = [\sum w(F_o^2 - F_c^2)^2 / \sum w(F_o^2)^2]^{1/2}.$$

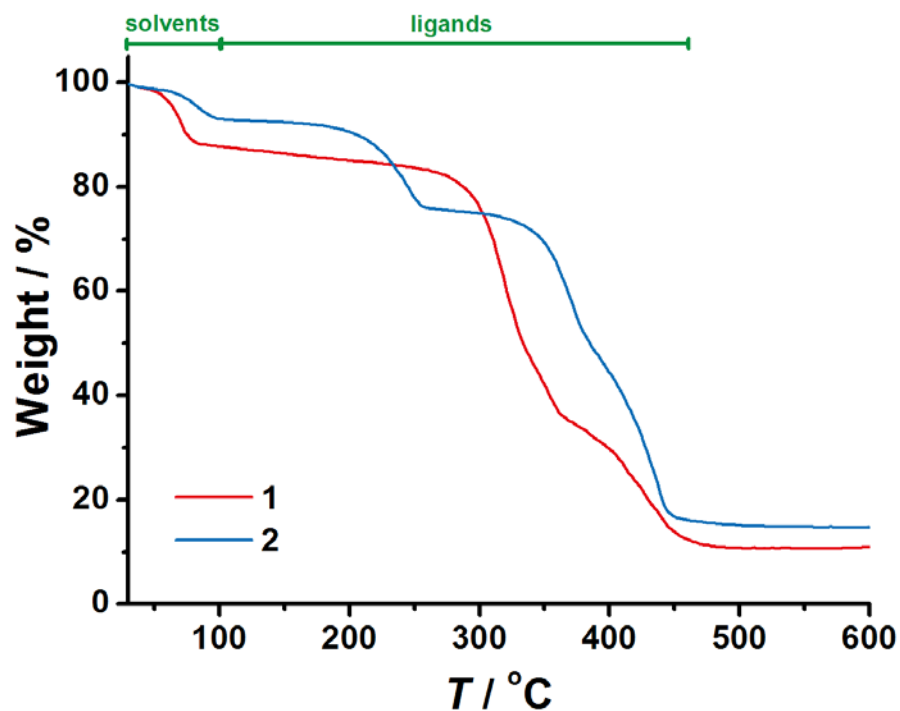


Figure S3. Thermogravimetric analysis of 1 (red) and 2 (blue) under N₂ atmosphere.

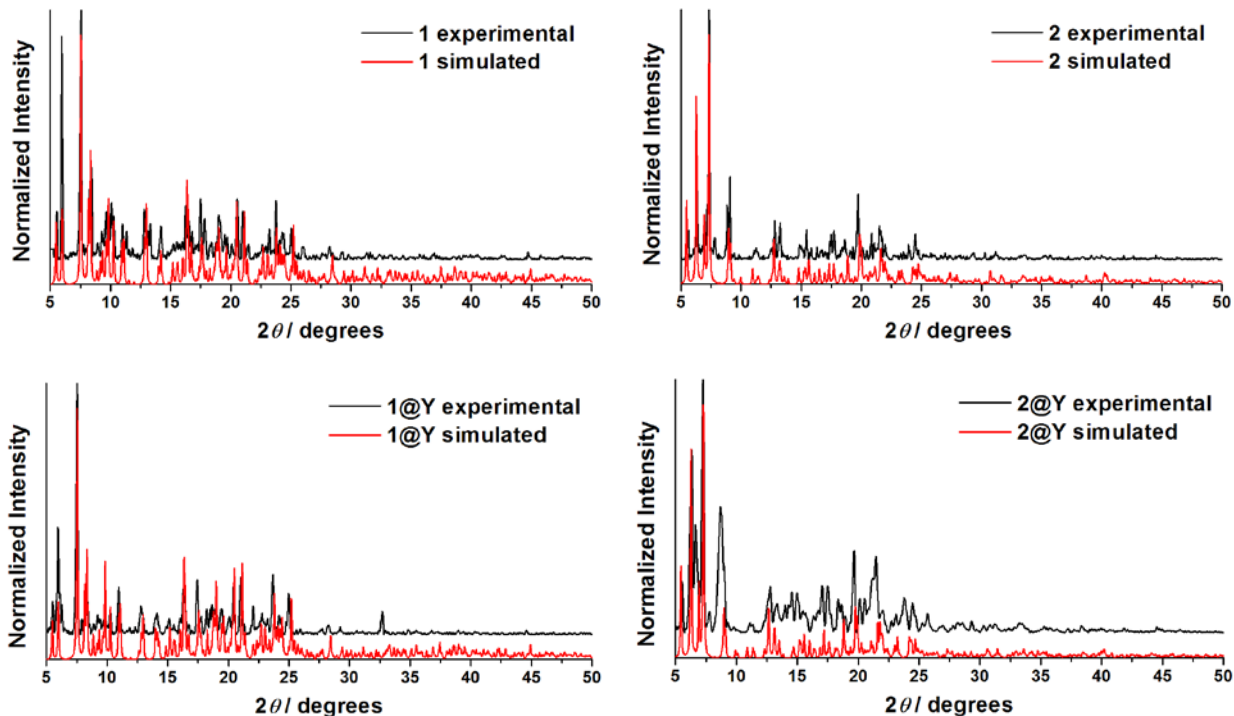


Figure S4. PXRD patterns of 1, 2, 1@Y and 2@Y compared with the simulated pattern from the single crystal structure.

2. Magnetic Characterization

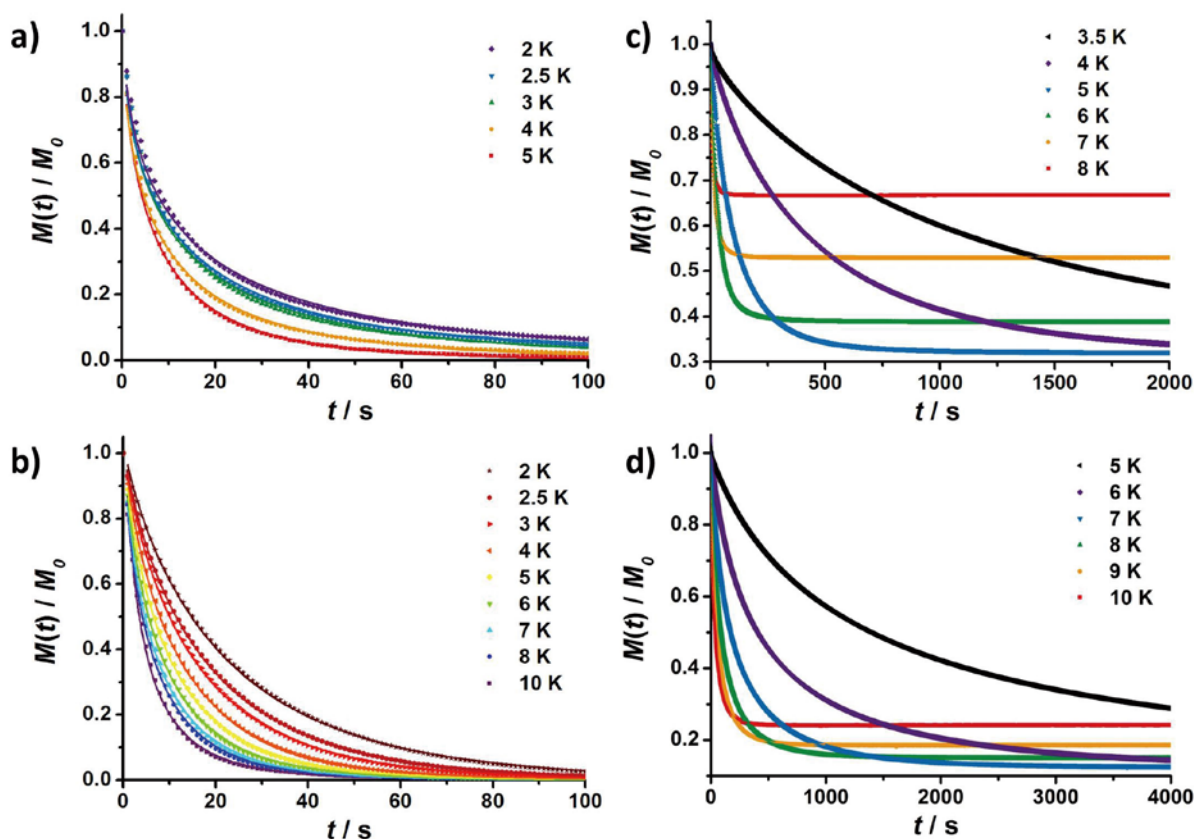


Figure S5. DC relaxation of 1 (a, c) and 2 (b, d) with the final field of 0 Oe (a, b) and 1 kOe (c, d). The magnetizations are plotted as normalized to M_0 (the starting value at $t = 0$) for clarity. The solid lines are the best fit to the exponential decay as $M(t) = M_f + (M_i - M_0) \exp[-(t/\tau)^\beta]$, where τ is the relaxation time. Note the different scale of the time axis (x).

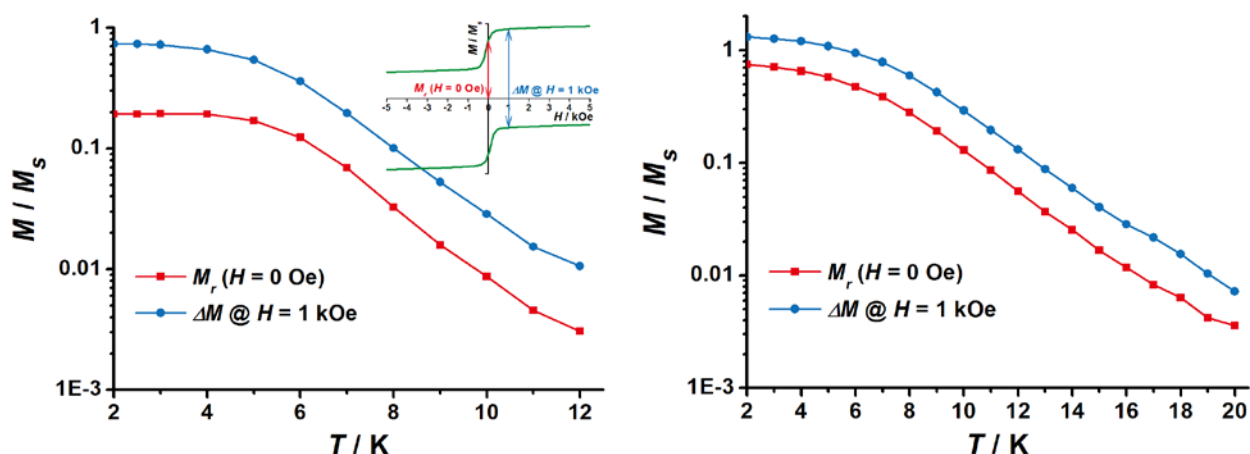


Figure S6. Temperature dependence of the remnant magnetization (M_r) at $H = 0$ Oe and the opening of the hysteresis loops (ΔM) at $H = 1$ kOe for 1 (left) and 2 (right). The magnetizations are normalized to the saturated magnetization (M_s) and the inset shows the schematic explanation of these two parameters. All lines are guides to the eyes.

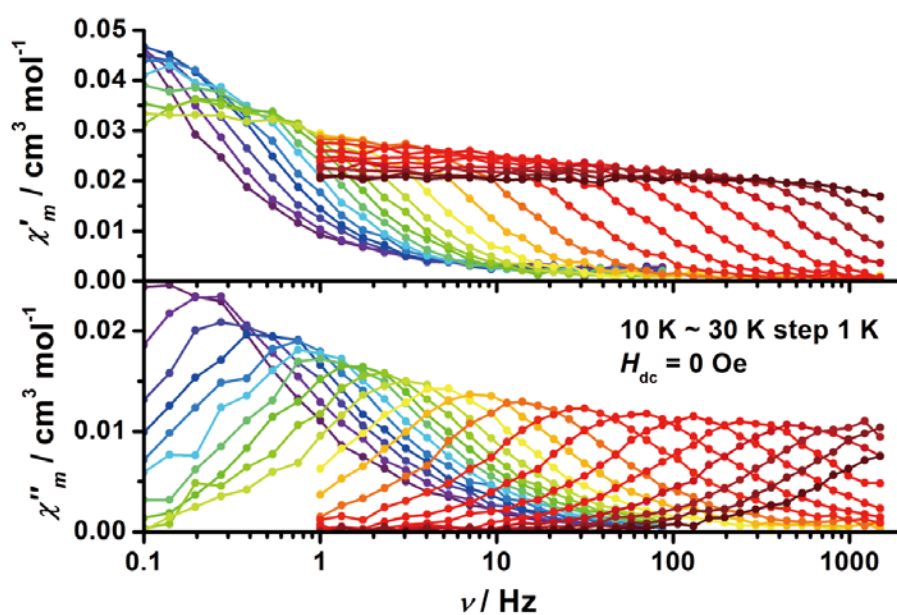


Figure S7. Frequency dependence of the alternating-current molar magnetic susceptibilities for 1@Y in zero dc field. Lines are guides to the eyes.

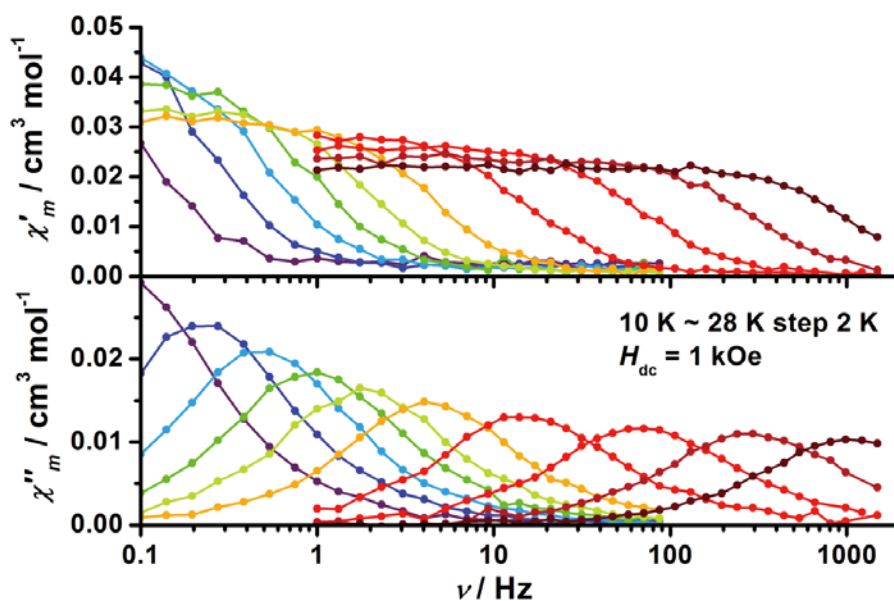


Figure S8. Frequency dependence of the alternating-current molar magnetic susceptibilities for 1@Y in 1 kOe dc field. Lines are guides to the eyes.

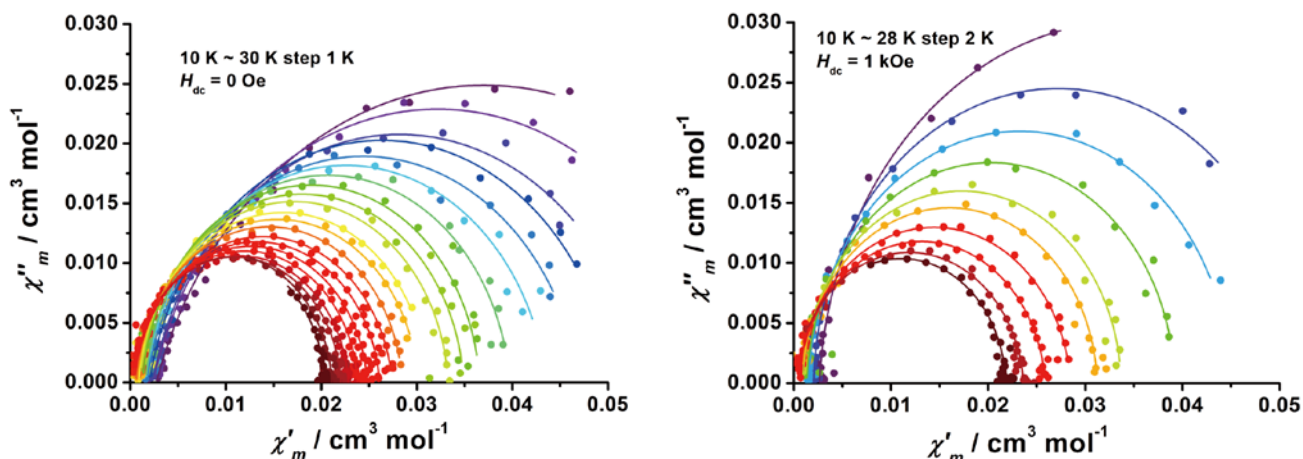


Figure S9. Cole-Cole plots for the ac susceptibilities for 1@Y in zero dc field (left) and in 1 kOe dc field (right). The solid lines are the best fit to the Debye's law.

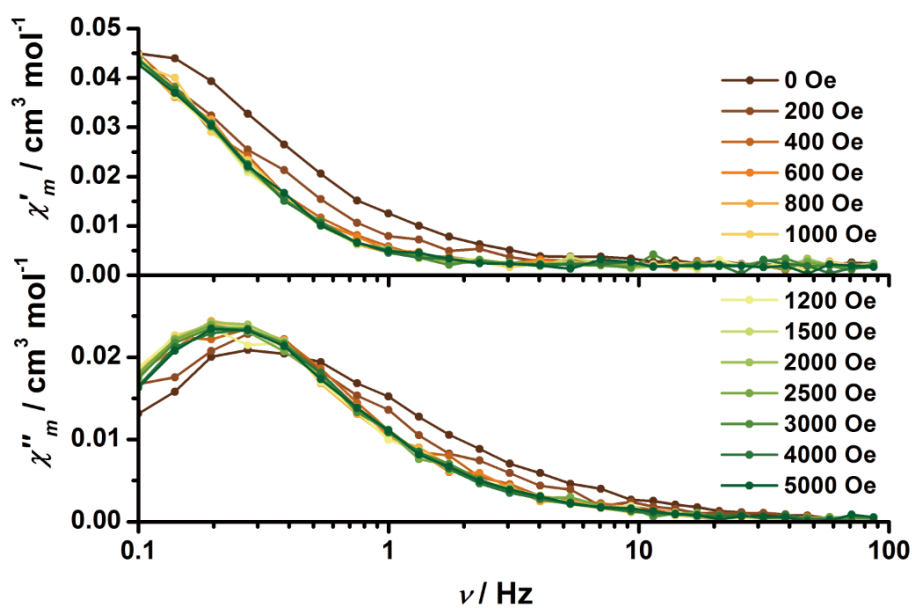


Figure S10. Field dependence of the alternating-current molar magnetic susceptibilities for 1@Y at 12 K. Lines are guides to the eyes.

3. Ab Initio Calculations

Table S4. Spin-orbital energies and corresponding g tensors of the **2-no-water** model system (The structure of the model compound **2-no-water** is identical to the structure of **2**, in which the five coordinated water molecules of the Dy site were removed from the *ab initio* calculations (vide infra) while all bromide counter-ions and Cy_3PO ligands were present.). Note the large excitation energies and the very small values of the g_x and g_y of the four low-lying Kramers doublets.

2-no-water			
Energy (cm ⁻¹)	g_x	g_y	g_z
0	1.65×10^{-7}	2.41×10^{-7}	19.91
520	0.32×10^{-8}	1.80×10^{-7}	17.01
1004	7.33×10^{-6}	7.60×10^{-6}	14.19
1377	7.91×10^{-4}	8.74×10^{-4}	11.54
1593	0.61	0.85	8.76
1654	2.17	6.18	13.27
1692	1.41	3.74	14.49
1732	2.13×10^{-2}	0.21	19.22

Table S5. Some magneto-structural correlations in the investigated compounds. Angles between the main anisotropy axis and the shortest chemical bond (degrees).

Contraction	1	2	2-no-water
Angles between the main anisotropy axis and the shortest chemical bond (O1)	0.44	3.05	0.90
Angles between the main anisotropy axis and the O1-O2 direction	2.42	3.28	0.51

Table S6. Angles between main anisotropy axes of the low-lying Kramers doublets.

Compound 1:

	1	2	3	4
1	0.00	2.56	88.12	86.76
2	2.56	0.00	85.56	84.92
3	88.12	85.56	0.00	41.68
4	86.76	84.92	41.68	0.00

Compound 2:

	1	2	3	4
1	0.00	89.43	3.35	87.43
2	89.43	0.00	86.87	6.18
3	3.35	86.87	0.00	84.67
4	87.43	6.18	84.67	0.00

Compound 2-no-water:

	1	2	3	4	5	6
1	0.00	0.10	0.40	1.68	7.25	88.27
2	0.10	0.00	0.35	1.67	7.28	88.38
3	0.40	0.35	0.00	1.32	6.96	88.31
4	1.68	1.67	1.32	0.00	5.70	87.80
5	7.25	7.28	6.96	5.70	0.00	83.93
6	88.27	88.38	88.31	87.80	83.93	0.00